

## CORRELATIONS OF RATES OF INSULIN RELEASE FROM ISLETS AND PLATEAU FRACTIONS FOR $\beta$ -CELLS

- ROBERT M. MIURA  
Department of Mathematics and Institute of Applied Mathematics,  
University of British Columbia,  
Vancouver, British Columbia,  
Canada V6T 1Z2  
*(E.mail:miura@neuron.math.ubc.ca)*

- MARK PERNAROWSKI  
Department of Mathematical Sciences,  
Montana State University,  
Bozeman, Montana 59717, U.S.A.  
*(E.mail:pernarow@mathfs.math.montana.edu)*

Pancreatic  $\beta$ -cells in intact islets of Langerhans perfused with various glucose concentrations exhibit periodic bursting electrical activity (BEA) consisting of active and silent phases. The fraction of the time spent in the active phase is called the plateau fraction and appears to be strongly correlated with the rate of release of insulin from islets as glucose concentration is varied. Here this correlation is quantified and a theoretical development is presented in detail. Experimental rates of insulin release are correlated with “effective” plateau fractions over a range of glucose concentrations. There are a number of different models for BEA in pancreatic  $\beta$ -cells and a method is developed here to quantify the dependence of a glucose dependent parameter on glucose concentration. As an example, the plateau fractions computed from the Sherman-Rinzel-Keizer model are matched with experimental plateau fractions to obtain a relationship between the model’s glucose-dependent parameter,  $\beta$ , and glucose concentration. Knowledge of the relationships between  $\beta$  and glucose concentration and between experimental measurements of rates of insulin release and plateau fractions permits the determination of theoretical rates of insulin release from the model.

**1. Introduction.** Bursting electrical activity (BEA) in excitable cells is associated with rapid action potential-like oscillations of the membrane potential and has been observed in neurons (Strumwasser, 1968) and more recently in endocrine cells such as pancreatic  $\beta$ -cells (Dean and Matthews, 1970a,b; Atwater *et al.*, 1978a,b; Meissner and Preissler, 1980; Henquin and Meissner, 1984). Synchronized BEA exhibited by pancreatic  $\beta$ -cells in intact islets of Langerhans is associated with the release of insulin from these islets (Dean and Matthews, 1970a,b; Meissner and Preissler, 1979; Scott *et al.*, 1981; Wollheim and Pralong, 1990). The BEA in  $\beta$ -cells is a periodic phenomenon consisting of successive active and silent phases. The active phase (or plateau) is characterized by rapid membrane voltage oscillations and the silent phase by slow voltage changes. The plateau fraction,  $\rho$ , is defined as the ratio of the duration of the active phase to the period of the BEA cycle. For normal  $\beta$ -cells under standard conditions, the plateau fraction has been (linearly) correlated to the rate of release of insulin as the glucose concentration is varied (Meissner and Schmelz, 1974; Ozawa and Sand, 1986).

One of the objectives in this paper is to quantify the relationship between experimentally measured rates of insulin release and plateau fractions. The biological mechanisms relating these quantities are still not fully understood. Existing data for rates of insulin release from islets of Langerhans and plateau fractions from  $\beta$ -cells in mouse are plotted in Figure 1. These data are sparse and there is a clear need for further experiments.

Existing biophysical models to describe BEA in pancreatic  $\beta$ -cells incorporate a variety of membrane ionic currents and intracellular ionic concentrations (Atwater *et al.*, 1980; Cook, 1984; Satin and Cook, 1988, 1989; Ashcroft and Rorsman, 1989; Henquin, 1990a,b; Hopkins *et al.*, 1991; Cook *et al.*, 1991). Depending on the model, the ionic currents are of Hodgkin-Huxley type and/or Goldman-Hodgkin-Katz type. The original “minimal” mathematical model proposed by Chay and Keizer (1983) was based loosely on the Hodgkin and Huxley (1952) model of the squid giant axon. Other models, such as that proposed by Sherman, Rinzel, and Keizer (SRK) (Sherman *et al.*, 1988) incorporated measurements from the voltage-clamp experiments of Rorsman and Trube (1986). In these earlier (first generation) models, intracellular calcium concentration is the slow variable responsible for triggering the

Figure 1a: Insulin(ng/hr/islet)

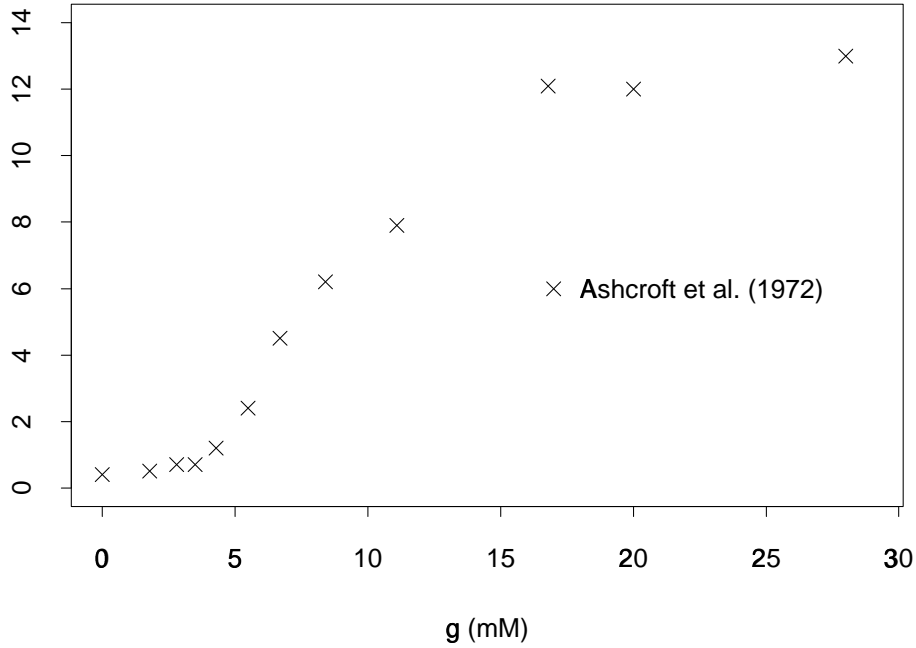


Figure 1b: Plateau Fractions

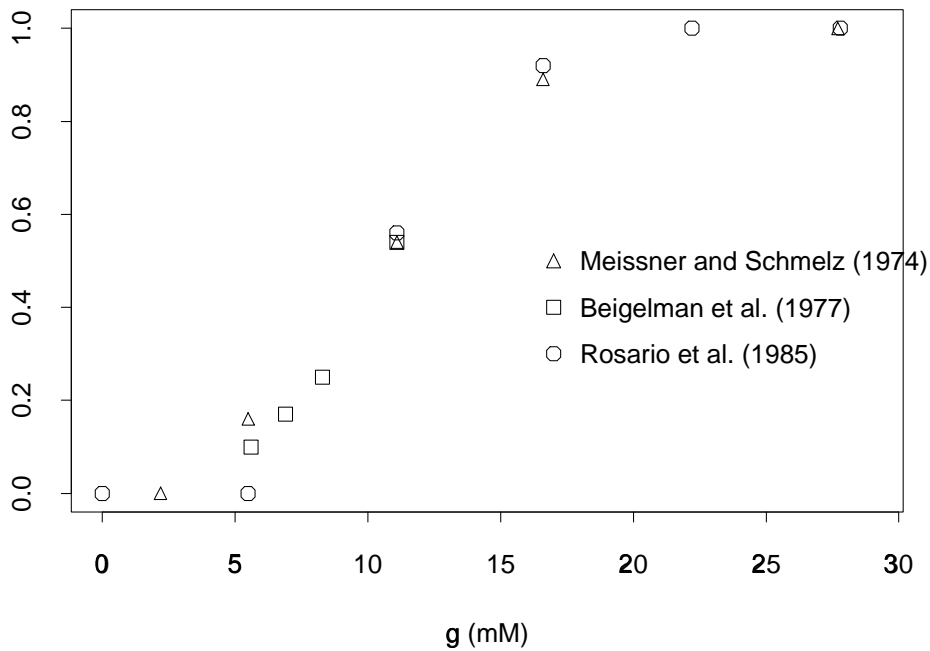


FIG. 1. Insulin release rates and plateau fractions in  $\beta$ -cell islets. (a) Experimental rate of insulin release as a function of glucose concentration. (b) Experimental plateau fractions as a function of glucose concentration. Data taken from authors indicated in legends, cf. Table 1.

transitions between the silent and active phases of the BEA cycle.

Although there is recent experimental evidence which seem to rule out the important roles of intracellular calcium accumulation Valdeolmillos *et al.* (1989) and  $Ca^{2+}$ -activated  $K^+$  channels (Henquin, 1990a,b; Bokvist *et al.*, 1990; Fatherazi and Cook, 1991) in BEA, consensus on this issue has not yet been reached. Thus there is a need for further experimentation as well as model development to accurately describe the biophysical mechanisms leading to BEA (Cook *et al.*, 1991). A (second generation) model based, in part, on these recent experimental findings has been proposed by Keizer and Smolen (1991). Regardless of the model, the functional relationship between the glucose parameter(s) and glucose concentration has not been accurately quantified. Therefore, another objective of this study is to show how to make explicit correlations between the glucose-dependent parameter in the models of BEA and rate of insulin release, i.e., on glucose concentration. This may help to determine the range of glucose concentrations over which the models are valid.

Experimental data (Beigelman *et al.*, 1977) indicate that  $\beta$ -cells do not exhibit BEA below a certain threshold glucose concentration (cf. Figure 1 and Table 1) and that above a specific higher glucose concentration there is a range of glucose over which all cells in an islet exhibit BEA. Above the threshold glucose concentration the electrical activity of the islet is characterized by an “effective” plateau fraction, i.e., the average plateau fraction over all  $\beta$ -cells in the islet, be they active or not. The basic underlying assumption for our theoretical treatment is that for each islet there is a functional (empirical) relationship between the rate of insulin release and the effective plateau fraction.

Other experimental evidence indicate that BEA can be dissociated from insulin release (Atwater *et al.*, 1984; Gembal *et al.*, 1992; Gilon *et al.*, 1993), i.e., that BEA is observed but insulin secretion is inhibited or abolished. This, however, does not contradict the existence of a correlation between BEA and insulin release in normal  $\beta$ -cells.

Here, our quantitative examination of the existing data (cf. Figure 1 and Table 1) for rate of release of insulin (Ashcroft *et al.*, 1972) and for plateau fractions (Meissner and Schmelz, 1974; Beigelman *et al.*, 1977; Rosario *et al.*, 1985) leads us to the following conclusions: 1) there is a residual rate of insulin release that is not correlated to BEA, 2) the relationship

between the BEA-dependent rate of release of insulin and effective plateau fraction is sigmoidal, 3) the relationship between rate of insulin release and glucose concentration is not sigmoidal, and 4) there presently is insufficient (quantitative) experimental data to completely test our theoretical correlations. Furthermore, there exists a gap in the experimental data for both insulin release rates and plateau fractions for glucose concentrations between 11 and 16 mM. In this range, the SRK model exhibits chaotic behavior.

Table 1. Experimental data

$g$ (mM)	Ashcroft <i>et al.</i> *	Meissner and Schmelz <sup>‡</sup>	Beigelman <i>et al.</i> <sup>§</sup>		Rosario <i>et al.</i> <sup>  </sup>
	$I$ (ng/hr/islet)	$\rho$	$\rho$	$A$	$\rho$
0.0	0.4				0.00
1.8	0.5				
2.2		0.00			
2.8	0.7				
3.5	0.7				
4.2				0.000	
4.3	1.2				
5.5	2.4	0.16			0.00
5.6			0.10	0.185	
6.7	4.5				
6.9			0.17	0.455	
8.3			0.25	0.875	
8.4	6.2				
11.1	7.9	0.54	0.54		0.56
16.6		0.89			0.92
16.8	12.1				
20.0	12.0				
22.2					1.00
27.7		1.00			
27.8					1.00
28.0	13.0				
33.2					1.00

\* Figure 1 in Ashcroft *et al.* (1972)

<sup>‡</sup> Figure 5 in Meissner and Schmelz (1974)

<sup>§</sup> Text of Beigelman *et al.* (1977)

<sup>||</sup> Figure 3 in Rosario *et al.* (1985)

**2. Theoretical Development.** In this section, we present the assumptions and theory necessary to correlate experimentally measured rates of insulin release from islets and plateau fractions of  $\beta$ -cells. Using this correlation and the plateau fractions computed from models

which describe BEA of  $\beta$ -cells, a theoretical prediction for the insulin release rate can be obtained. The assumptions concerning the dependence of both the insulin release rate of islets and plateau fractions on glucose are clearly defined. Furthermore, a method for determining the functional dependence of a parameter in the BEA models on glucose concentration is described. A specific application to experimental data of the correlation techniques described here is given in Section 3.

2.1. *Insulin release and effective plateau fraction.* We consider a single intact islet which contains  $N$   $\beta$ -cells. Each  $\beta$ -cell has a plateau fraction,  $\rho_i$ ,  $i = 1, 2, \dots, N$ , which depends on the cell's individual characteristics and the glucose concentration,  $g$ . As noted earlier, for glucose concentrations below a certain threshold level, say  $g_t$ , experiments indicate  $\beta$ -cells are inactive, i.e., they are not exhibiting BEA and, by definition, have a plateau fraction equal to zero. For glucose concentrations above  $g_t$ , the number of  $\beta$ -cells undergoing BEA increases until all the cells are bursting in synchrony (Beigelman *et al.*, 1977), i.e., there is a range of glucose concentrations over which the threshold for bursting of individual  $\beta$ -cells varies. The nonsynchronous behavior of  $\beta$ -cells for glucose concentrations just above threshold is due partly to coupling effects between the cells, local glucose variations, and inhomogeneities in the cell properties. At high glucose concentrations,  $\beta$ -cells spike continually (no silent phase) in which case their plateau fractions are defined to be equal to one.

To characterize the BEA of an islet, we define the effective plateau fraction by

$$(1) \quad \rho_f \equiv \frac{1}{N} \sum_{i=1}^N \rho_i.$$

This expression can be rewritten as

$$(2) \quad \rho_f = \frac{N_a}{N} \cdot \left( \frac{1}{N_a} \sum_{i=1}^N \rho_i \right) \equiv A \cdot \bar{\rho},$$

where  $N_a$  is the number of active (or bursting) cells,  $A = N_a/N$  is the fraction of active cells, and  $\bar{\rho}$  is the average plateau fraction of all those cells which are undergoing BEA. The distinction between  $\rho_f$  and  $\bar{\rho}$  reflects the difference between the collective and individual average behavior of  $\beta$ -cells in an islet. Either of these quantities can be obtained experimentally by keeping track of those cells that are exhibiting BEA and those that are not. For example, Beigelman *et al.* (1977) report  $\rho_i$ ,  $\bar{\rho}$ , and  $A$  at different glucose concentrations. The latter two can be used to compute  $\rho_f$ .

The insulin release rate of the islet,  $I$ , will be correlated with the effective plateau fraction. The assumptions (consistent with existing experimental data) underlying this correlation are summarized below:

(A1) There are three glucose concentrations  $g_t < g_a < g_s$  such that

- a) All  $\beta$ -cells within the islet are inactive if  $0 \leq g \leq g_t$ .
- b) For glucose concentrations in the range  $(g_t, g_a)$ , the fraction,  $A$ , of active (bursting)  $\beta$ -cells increases from zero to one.
- c) For concentrations above  $g_s$ , all  $\beta$ -cells are spiking continuously.

(Note that we have omitted any statement about what happens in the range  $g_a \leq g < g_s$ . A further discussion of this range of glucose concentrations is given later.)

(A2) The insulin release rate of the islet,  $I$ , is given by the sum

$$(3) \quad I = I_{res}(g) + I_{BEA}(g) \quad ,$$

where  $I_{res}$  is the residual release rate not correlated with the BEA and  $I_{BEA}$  is the release rate correlated with the BEA. For glucose concentrations below the threshold,  $g_t$ ,  $I = I_{res}$ .

(A3) There is a functional (empirical) relationship between the insulin release rate,  $I_{BEA}$ , and the effective plateau fraction,  $\rho_f$ . We assume that this relationship is given by the general nonlinear expression

$$(4) \quad I_{BEA} = \bar{I}_{BEA} R(\rho_f) \quad ,$$

where  $\bar{I}_{BEA}$  is the maximum of  $I_{BEA}(g)$  over all glucose concentrations, hence  $0 \leq R(\rho_f) \leq 1$ . The functional dependence of  $R$  on  $\rho_f$  is to be determined. Note that the function  $R$  is the normalized insulin release rate correlated with BEA, i.e.,

$$(5) \quad R = \frac{I - I_{res}}{\bar{I}_{BEA}} \quad .$$

The quantities defined in these assumptions can be determined by an experimental correlation of insulin release rates and effective plateau fraction values measured at the same glucose concentrations. First, measure the insulin release rates,  $I_m$ , and the corresponding plateau fractions,  $\rho_m$ , at the glucose concentrations  $g_m$ ,  $m = 1, 2, \dots, M$ . The threshold glucose concentration,  $g_t$ , is then determined as the maximum glucose concentration for which all cells are inactive.

To determine the functional dependence of the residual release rate on glucose concentration, first choose a functional form  $I_{res}(g; \vec{\kappa})$  where  $\vec{\kappa} = (\kappa_1, \kappa_2, \dots, \kappa_P)$  are fitting parameters. Values for these parameters are subsequently found by using the measured insulin release rates with  $g < g_t$ . (Isolating  $I_{res}$  by pharmacologically suppressing the BEA would yield more satisfactory results.) The maximal release rate,  $\bar{I}_{BEA}$ , is then found as the maximum value of the difference  $I_m - I_{res}(g_m; \vec{\kappa})$  among all the glucose concentrations,  $g_m$ ,  $m = 1, 2, \dots, M$ .

The corresponding effective plateau fractions,  $\rho_{f_m}$ ,  $m = 1, 2, \dots, M$ , at the glucose concentrations,  $g_m$ , must be computed from the measured plateau fractions, either  $\rho_i$  or  $\bar{\rho}$ , at



the same concentrations. The range of these concentrations must be broad enough so that at some concentrations no cells are bursting while at other (higher) concentrations all cells are in the continuous spiking mode. If, as in Beigelman *et al.* (1977), experimental values of the fraction of active cells,  $A_m$ , are reported at different  $g_m$  values,  $A$  may be regarded as a function of the glucose concentration. Choosing a functional form  $A = A(g; \vec{\mu})$  where  $\vec{\mu} = (\mu_1, \mu_2, \dots, \mu_Q)$  are fitting parameters, a subsequent correlation of the  $A_m$  and  $g_m$  values determines the vector  $\vec{\mu}$ . Once  $\vec{\mu}$  has been determined,  $\rho_f(g)$  can be computed from  $A(g; \vec{\mu})$  and  $\bar{\rho}(g)$  using (2).

Since the relationship defined in (4) is empirical, the functional form of  $R$  can be chosen arbitrarily (an example with a specific choice of  $R$  is given in Section 3). In general,  $R = R(\rho_f; \vec{\lambda})$  where  $\vec{\lambda} = (\lambda_1, \lambda_2, \dots, \lambda_\ell)$  are fitting parameters. The vector  $\vec{\lambda}$  is found from (4) by correlating effective plateau fractions with normalized BEA-dependent rates of insulin release computed from (5) using  $I_{res}(g; \vec{\kappa})$ ,  $\bar{I}_{BEA}$ , and experimentally measured insulin release rates. Then,  $\vec{\lambda}$  is determined through the correspondence

$$(6) \quad \frac{I_m - I_{res}(g_m)}{\bar{I}_{BEA}} = R(A(g_m; \vec{\mu})\bar{\rho}_m; \vec{\lambda}), \quad m = 1, 2, \dots, M.$$

In Section 3, we determine  $I_{res}(g; \vec{\kappa})$ ,  $A(g; \vec{\mu})$ , and  $R(\rho_f, \vec{\lambda})$  using data published in the literature.

*2.2. Theoretical rates of insulin release.* In order for a mathematical model describing the BEA of  $\beta$ -cells to be relevant to insulin secretion, it must contain a glucose-dependent parameter, which we will refer to as  $\beta$ . The functional dependence of this parameter on glucose is not known. In this section, we determine the relationship between  $\beta$  and glucose concentration, and use this relationship to predict the theoretical rates of insulin release based on a mathematical model of BEA.

Typically, models of BEA in  $\beta$ -cells have the form

$$(7) \quad \frac{dv}{dt} = - \sum_{i=1}^q I_i(v, \vec{n}, \vec{c}; \beta) ,$$

$$(8) \quad \frac{dn_j}{dt} = \frac{N_j(v, \vec{c}) - n_j}{\tau_{n_j}(v)} \quad j = 1, 2, \dots, r ,$$

$$(9) \quad \frac{dc_k}{dt} = \varepsilon_k h_k(v, \vec{c}; \beta) \quad k = 1, 2, \dots, s ,$$

where  $v$  is the membrane potential,  $I_i$  are the ionic currents incorporated into a specific model,  $\vec{n} = (n_1, n_2, \dots, n_r)$  are relaxation variables which govern the voltage-gating of some of these currents,  $\vec{c} = (c_1, c_2, \dots, c_s)$  are concentrations of agents which regulate the BEA (e.g., intracellular calcium or ATP),  $h_k$  describes the buffering of agent  $c_k$ , and  $t$  is time. In the existing models, at least one of the parameters  $\varepsilon_k$  is small, hence the corresponding  $c_k$  varies slowly (see Pernarowski *et al.* (1992) and de Vries *et al.* (1994) for references to some of these other models).

For a particular mathematical model of BEA, the corresponding values of the plateau fraction will be denoted as  $\hat{\rho}$ . Our basic assumption relating these theoretical values to the experimental values is

$$(A4) \quad \hat{\rho} = \bar{\rho} ,$$

i.e., the average plateau fractions of active cells can be determined by numerically computing theoretical values for the plateau fraction. These theoretical values depend on  $\beta$ , i.e.,  $\hat{\rho} = \hat{\rho}(\beta)$ , which in turn depends on the glucose concentration.

If we assume a particular functional form for  $\beta$ , i.e.,  $\beta = \beta(g; \vec{\nu})$  where  $\vec{\nu} = (\nu_1, \nu_2, \dots, \nu_n)$  are fitting parameters, a correlation of the experimental values of the plateau fraction with the theoretical values of the plateau fractions in (A4) at different glucose concentrations will determine the vector  $\vec{\nu}$ . In many models,  $\beta$  is inversely proportional to the buffering rate,  $k_{Ca}$ , of intracellular calcium. Rinzel *et al.* (1986) suggest the functional relationship

$$(10) \quad k_{Ca} = k_{Ca}^* \frac{G^p}{1 + G^p} \quad ,$$

between  $k_{Ca}$  and  $g$  where  $G = g/g_m$  is a dimensionless glucose concentration (no values for  $p$  or  $g_m$  are suggested). This relationship represents unknown steady state chemical kinetics associated with the calcium buffering. Here we propose the more general formula

$$(11) \quad k_{Ca} = k_c + k_{Ca}^* \frac{(g - g_t)^p}{K + (g - g_t)^p}, \quad g_t \leq g < g_s .$$

The parameters  $k_{Ca}$ ,  $k_c$ , and  $k_{Ca}^*$  each have units of  $\text{msec}^{-1}$ ,  $K$  is a dissociation constant, and  $k_c$  is the value of  $k_{Ca}$  at the threshold concentration,  $g_t$ . Using this formula in conjunction with the mathematical model and correlating theoretical and experimental  $\bar{\rho}$  values, we can determine the parameter values,  $\vec{v} = (p, k_c, k_{Ca}^*, K, g_t)$ .

Once the functional dependence of  $\beta$  on glucose has been determined, the theoretical values of the plateau fraction,  $\hat{\rho}$ , can be used in place of  $\bar{\rho}$  in (2) to determine  $\rho_f$  which in turn is used in  $R$  to determine the normalized insulin release rates, cf. equation (6). Using  $I_{res}(g; \vec{k})$  and  $\bar{I}_{BEA}$  obtained from experimental data and  $R(\rho_f; \vec{\lambda})$ , the theoretical insulin release rates are obtained from (3) and (4).

**3. Experimental Correlations.** In this section, we illustrate the techniques presented in Section 2 to determine the correlation between insulin release rates and effective plateau fractions by applying them to existing data from islets of Langerhans taken from mouse. Since our objective is merely to demonstrate the applications of the procedure given in Section 2 and because there is little experimental data, most parameter fits have been done by eye rather than using accurate fitting procedures.

Assuming the linear relationship

$$(12) \quad I_{res}(g; \vec{\kappa}) = \kappa_1 + \kappa_2 g \quad ,$$

and using the release rate data from Ashcroft *et al.* (1972) for  $g < g_t \simeq 4.2$  mM, a linear regression yields the values  $\kappa_1 = 0.319$  and  $\kappa_2 = 0.197$ . Thus, using (12) in the definition of  $\bar{I}_{BEA}$  in assumption (A3), we obtain the value  $\bar{I}_{BEA} = 9.8$  ng/hr/islet from the release rate data reported by Ashcroft *et al.* (1972).

Existing data on plateau fractions come from measuring BEA in active cells within islets (Meissner and Schmelz, 1974; Beigelman *et al.*, 1977; Rosario *et al.*, 1985). These values are reported as the average quantities  $\bar{\rho}$ . In Beigelman *et al.* (1977), the fraction of active cells,  $A(g)$ , within the islets was estimated as a function of glucose. To match the four data points given in that reference, we choose the cubic form

$$(13) \quad A(g; \vec{\mu}) = \mu_1 x^3 + \mu_2 x^2 + \mu_3 x + \mu_4, \quad x = g - g_t + 4.2, \quad g_t \leq g \leq g_a,$$

with their suggested glucose threshold value  $g_t = 4.2$  mM. For the choices  $\vec{\mu} = (\mu_1, \mu_2, \mu_3, \mu_4) = (1.64 \times 10^{-3}, 2.95 \times 10^{-4}, 1.02 \times 10^{-2}, -0.170)$  and  $g_t = 4.2$  mM,  $A(g; \vec{\mu})$  goes through all four data points with  $A = 1$  at  $g_a = 8.6$  mM =  $g_t + 4.4$ . The fraction  $A(g)$  is zero for  $g \leq g_t$  and one for  $g \geq g_a$ . By keeping this same form and varying  $g_t$ , neither the response (shape) of  $A$  nor the range over which  $A$  increases from zero to unity changes. Other experiments measuring the plateau fraction of single  $\beta$ -cells at several glucose concentrations (Meissner and Schmelz, 1974; Beigelman *et al.*, 1977; Rosario *et al.*, 1985) indicate different values for the glucose threshold value,  $g_t$ . For the remainder of this paper, we use  $g_t = 5$  mM while fixing  $\vec{\mu}$  (cf. Figure 3).

Using (13), effective plateau fractions in (2) for a given glucose concentration now can be computed from the experimental  $\bar{\rho}$  values obtained from Meissner and Schmelz (1974),

Beigelman *et al.* (1977), and Rosario *et al.* (1985) by using the formula

$$(14) \quad \rho_f(g) = \begin{cases} 0 & 0 \leq g \leq g_t \\ A(g)\bar{\rho} & g_t < g < g_a \\ \bar{\rho} & g_a \leq g < g_s \\ 1 & g_s \leq g \end{cases}$$

where our choice of  $g_t = 5$  mM yields  $g_a = 9.4$  mM. In most cases, the glucose concentrations in these experiments were identical to those in the insulin release experiments of Ashcroft *et al.* (1972). In a few cases the glucose concentrations were not identical but were sufficiently close that we can match  $\bar{\rho}$  values from the plateau fraction experiments with insulin release rates from Ashcroft *et al.* (1972). From these matched pairs, we compute and plot the effective plateau fractions against the normalized BEA-dependent rates of insulin release. For each effective plateau fraction and insulin release rate pair plotted in Figure 2, the corresponding glucose concentrations differ by at most  $0.36 \mu\text{M}$ .

The points in Figure 2 give the experimental correspondence between the effective plateau fractions and the normalized BEA-dependent rates of insulin release,  $R$ , and this appears to be sigmoidal. Thus, we obtain a  $\rho_f$  vs  $R$  curve by fitting the function

$$(15) \quad \rho_f = \frac{1 + \tanh(\lambda_1(R - \lambda_2))}{2} ,$$

through these data points. The curve corresponding to (15) is superimposed on Figure 2 for the parameter values  $\vec{\lambda} = (\lambda_1, \lambda_2) = (6.0, 0.625)$ . As can be seen, this empirical correlation between the curve and the experimental data is excellent. Thus the simple linear relationship assumed in Ozawa and Sand (1986) should be replaced by a more accurate sigmoidal relationship as shown in Figure 2.

Given an experimental value of  $\bar{\rho}$ , the effective plateau fraction is computed from (14) and then the normalized BEA-dependent rate of insulin release is found by computing the

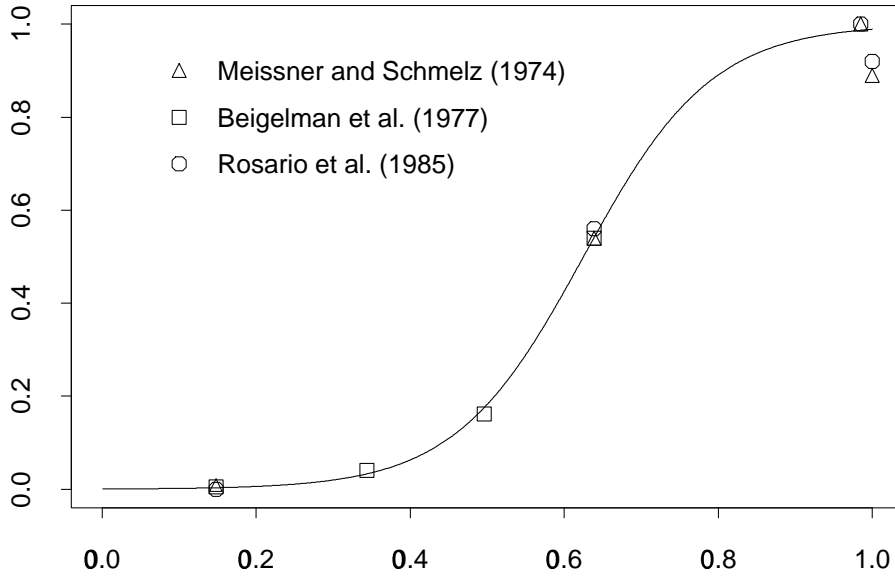


FIG. 2. *Effective plateau fraction as a function of normalized insulin release rate. Data taken from authors indicated in legends, cf. Table 1.*

inverse of (15), namely

$$(16) \quad R = \lambda_2 + \frac{1}{2\lambda_1} \ln\left(\frac{\rho_f}{1 - \rho_f}\right) \quad , \quad 0 < \rho_f < 1.$$

Thus, the insulin release rates in (4) can be computed from experimental plateau fractions via the relations defined in (13), (14), and (16).

**4. Example Using a Mathematical Model of BEA.** In this section, we illustrate how to use a mathematical model of BEA in  $\beta$ -cells to determine the dependence of both the glucose-dependent parameter and the theoretical rates of insulin release from an islet on glucose concentration. As a specific example, we use the SRK model (Sherman *et al.*, 1988) for which the nondimensionalized model equations have the form (7)-(9) with  $r = 1 = s$  (Pernarowski *et al.*, 1991). This model is representative of a class of models each of which

assume different ionic mechanisms. We stress that we use it here only to illustrate a procedure which is more generally applicable.

The time-dependent variables in the SRK model are the membrane potential of the cell,  $v$ , the activation variable for the voltage-sensitive potassium channel,  $n$ , and the intracellular cytoplasmic calcium concentration,  $c$ . The single dimensionless glucose-dependent parameter,  $\beta$ , occurs explicitly only in (9) and is inversely proportional to the dimensional glucose-dependent parameter,  $k_{Ca}$ , which is associated with the rate of calcium removal from the cytoplasm by pumps, mitochondrial uptake, or the endoplasmic reticulum.

For each value of  $k_{Ca}$ , the differential equations can be integrated numerically and a theoretical plateau fraction,  $\hat{\rho}$ , computed (Pernarowski *et al.*, 1992). As  $k_{Ca}$  is increased from 0.005 to 0.05 msec<sup>-1</sup>, the qualitative behavior of the solution of (7)-(9) changes from steady state to bursting to continual spiking (cf. Figure 3). Since an increase in glucose concentration is represented by an increase in  $k_{Ca}$ , the model equations correctly describe the qualitative dependence of the electrical behavior of the  $\beta$ -cell on  $g$ . In addition to these different behaviors, the model equations exhibit chaotic motion for  $k_{Ca}$  near the value where the transition from bursting to continual spiking takes place.

For each choice of  $\vec{v}$ , the corresponding  $\hat{\rho}$  vs  $k_{Ca}$  curve can be converted into a  $\hat{\rho}$  vs  $g$  curve via (11) and then compared with experimental  $\bar{\rho}$  values. Several different  $p$  values,  $p = 1, 2, 3, 4$ , were used for these comparisons. For  $p = 1$ , it was found that the correlation between the theoretical plateau fraction curve and experimental values was best for large values of  $K$  (in the range 280-340  $\mu$ M). The best fit was obtained for  $p = 3$  while noninteger values of  $p$  near three resulted in poorer fits.

Theoretical values for the plateau fraction were computed using the SRK model and employing assumption (A4). In Figure 3, the theoretical  $\hat{\rho}$  vs  $g$  curve corresponding to  $p = 3$  is compared to the plateau fractions measured by Meissner and Schmelz (1974), Beigelman *et al.* (1977), and Rosario *et al.* (1985). Parameter values for the theoretical curve  $\hat{\rho}$  vs  $g$  curve shown in Figure 3 are  $\vec{v} = (p, k_c, k_{Ca}^*, K, g_t) = (3, 0.023, 0.029, 65, 5)$ . It can be seen from the figure that theoretical and experimental values compare favorably. Chaotic behavior observed in solutions of the model equations occurred in the range of  $g$  between the vertical

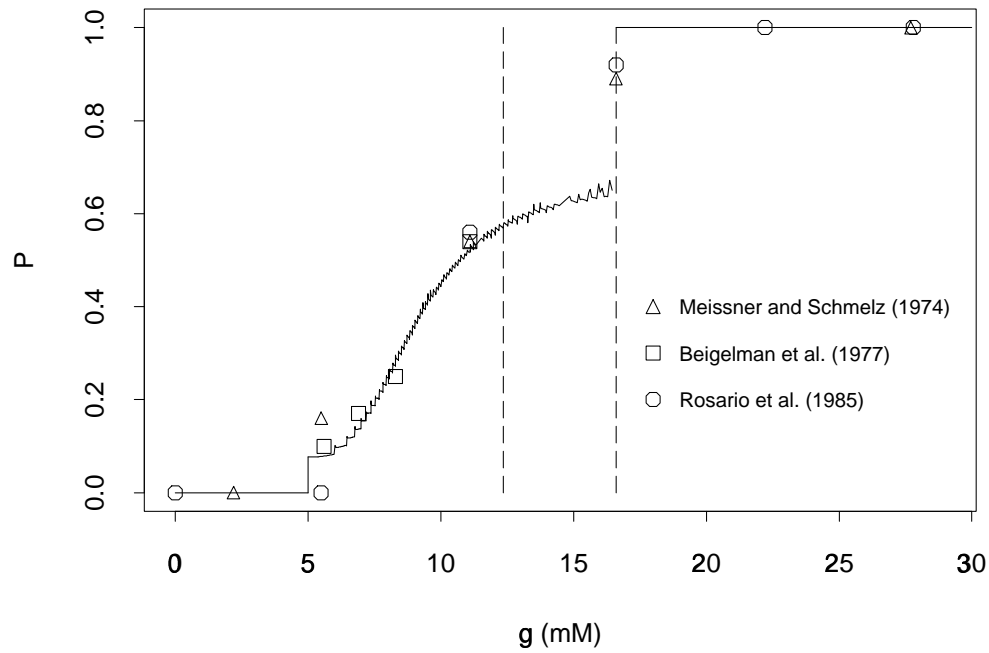


FIG. 3. Plateau fractions as a function of glucose concentration. Solid lines indicate theoretically obtained values for  $\hat{p}$  from the SRK model. Note the jumps in both the experimental and theoretical values of the plateau fraction at  $g_t = 5$  mM and  $g_s = 16.6$  mM. Solutions of the SRK equations exhibited chaotic behavior for glucose values between the vertical dashed lines. Relationship between the glucose concentration,  $g$ , and the buffering rate,  $k_{Ca}$ , is approximated by (11) using  $p = 3$ . Data taken from authors indicated in legends, cf. Table 1.



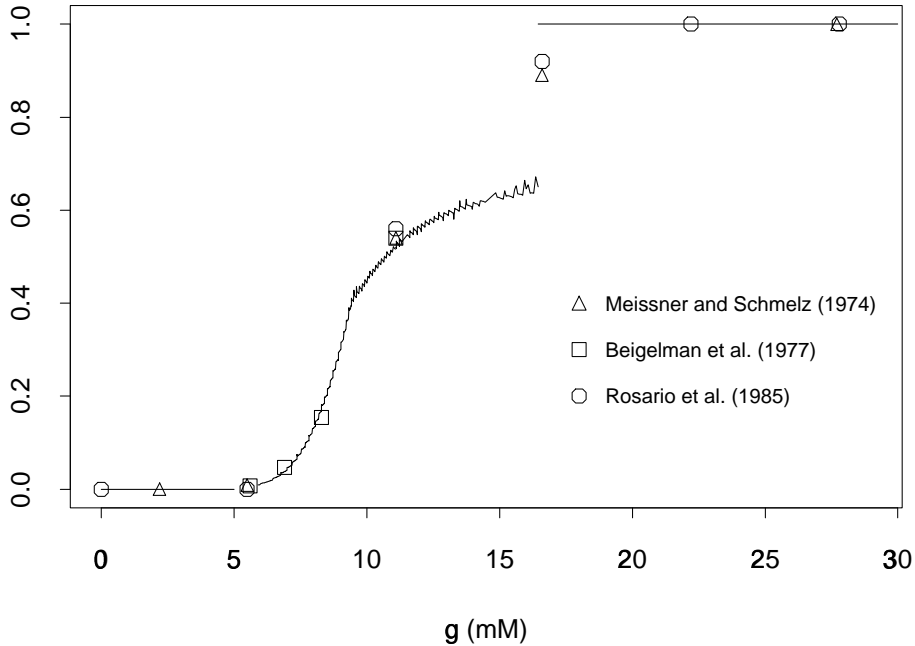


FIG. 4. *Effective plateau fraction as a function of glucose concentration. For the case  $p = 3$ , the effective plateau fraction,  $\rho_f$ , for the SRK model is plotted against glucose concentration. The difference between this graph and the graph in Figure 3 occurs in the glucose range 5 to 9.4 mM where the multiplicative factor  $A$  in (2) increases from zero to one. Data taken from authors indicated in legends, cf. Table 1.*

dashed lines. The jaggedness in the theoretical curve reflects some of the fine structure embodied in the solutions of the model equations. For the parameter values  $\vec{\nu}$  used in Figure 3, the SRK model predicts  $g_s = 16.6$  mM for the glucose concentration at which  $\beta$ -cells make the transition from bursting to continuous spiking. However, since the experimental data used to determine  $\vec{\nu}$  are sparse, it is difficult to assess the accuracy of such a prediction.

Theoretical values for the effective plateau fraction were computed from (14) by using the  $\vec{\nu}$  values in Figure 3 and the  $\vec{\mu}$  values used to define  $A$  in (13). The resulting  $\rho_f$  vs  $g$  curve is shown in Figure 4. Also superimposed on this figure are effective plateau fractions computed from Meissner and Schmelz (1974), Beigelman *et al.* (1977), and Rosario *et al.* (1985). The difference between the results in Figures 3 and 4 is the effect of the multiplicative factor  $A(g)$  which only changes the shape of the  $\hat{\rho}$  curve in the glucose range  $(g_t, g_a)$ . Whereas there is a jump in the value of  $\hat{\rho}$  at  $g_t$ , there is a smooth transition in the  $\rho_f$  curve at  $g_t$ .

Finally, the theoretical  $\rho_f$  values computed from the SRK model can be used to evalu-

ate theoretical normalized BEA-dependent rates of insulin release,  $R$ , via (16). Using these normalized release rates, the fit in (12), and the value  $\bar{I}_{BEA} = 9.8$  ng/hr/islet, theoretical rates of insulin release  $I$  can be computed and compared to experimental results. Such a comparison is shown in Figure 5, where parameter values used to construct Figure 4 were used to compute theoretical insulin release rates from the SRK model. Superimposed on this figure are the experimental data of Ashcroft *et al.* (1972). Also, effective plateau fractions computed from Meissner and Schmelz (1974), Beigelman *et al.* (1977), and Rosario *et al.* (1985) were used in (4) to compute corresponding normalized insulin release rates. The agreement between the experimental values and theoretical curves is very good, especially for glucose concentrations  $g < g_s = 16.6$  mM. For  $\rho_f = 1$ , a good approximation of (3) is given by

$$(17) \quad I = I_{res}(g) + \bar{I}_{BEA}, \quad g > g_s,$$

since  $R \simeq 1$ . The fit (12) of  $I_{res}$  only used data with glucose concentrations  $g < g_t$ , thus the interpolated values for  $I$  in (17) yield larger errors in Figure 5 for  $g > g_s$ .

**5. Discussion.** In this paper, we have proposed methods: 1) to quantify the relationship between the rate of release of insulin from islets of Langerhans and the plateau fractions measured for  $\beta$ -cells as a function of glucose concentration, and 2) to determine the dependence of a parameter in models of BEA in  $\beta$ -cells on glucose concentration. Combining the results obtained by applying these two methods, models of BEA in  $\beta$ -cells can be used to predict theoretical insulin release rates. These methods have been illustrated on existing data from mouse for rates of insulin release and plateau fractions, and on the SRK model of BEA in  $\beta$ -cells. Until a generally accepted model for  $\beta$ -cell BEA is formulated, the precise role that particular ionic channels have on BEA-dependent insulin release remains unknown. We stress that the procedure for determining such roles via assumption (A4) is model independent.

From the experimental data, an empirical correlation between the rate of release of insulin from an islet and the effective plateau fraction obtained from measured plateau fractions of

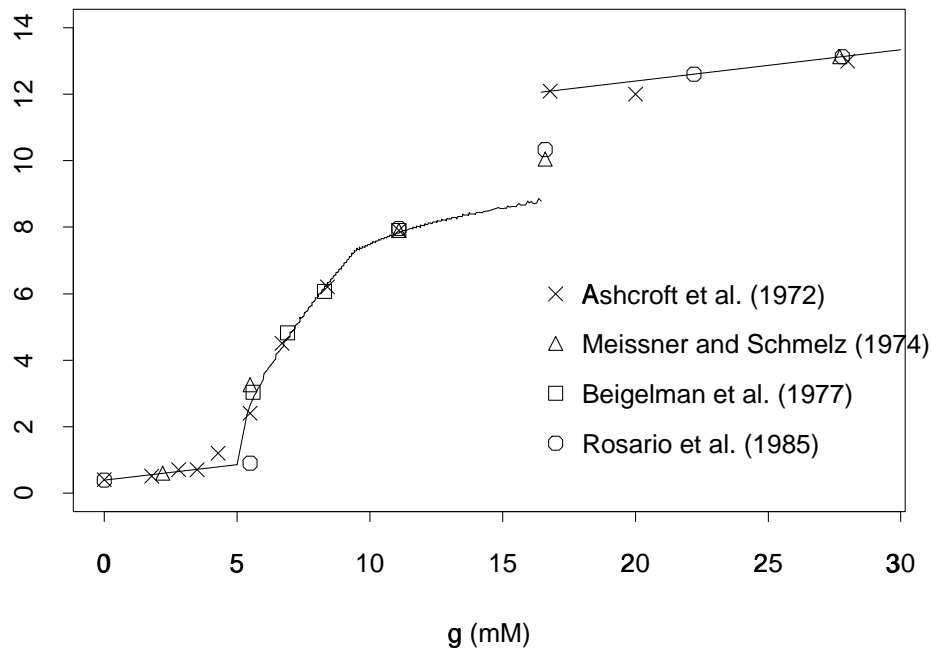


FIG. 5. Experimental and theoretical insulin release rates obtained from experimental and theoretical plateau fractions. Solid lines indicate release rates obtained using plateau fractions computed from the SRK model of BEA in  $\beta$ -cells. Data taken from authors indicated in legends, cf. Table 1.

individual cells is achieved by a simple sigmoidal relationship. However, the existing data are insufficient to completely test the methods proposed here. In this regard, there are two relevant issues. Firstly, the residual rate of insulin release,  $I_{res}$ , could be measured directly in experiments where pharmacological blockers are used to suppress the BEA. The assumption in (12) that this residual rate depends linearly on glucose concentration was based on four data points over a narrow range of  $g$  in which release rates were low and difficult to measure. Secondly, the gap between the glucose concentrations in the range 11-16  $\mu\text{M}$  at which the insulin release rates and the plateau fractions were measured is significant because models of BEA can exhibit solutions with some chaotic behavior inside this range.

Ultimately, insulin release rates predicted from a model of BEA in  $\beta$ -cells will depend on the assumptions used to formulate the model. The SRK model used in Section 4 to compute theoretical insulin release rates predicts a slow “sawtooth” oscillation in the intracellular  $\text{Ca}^{2+}$  concentrations during the active phase. In contrast, intracellular  $\text{Ca}^{2+}$  concentrations measured by Santos *et al.* (1991) have a square-wave appearance and the recent model by Smolen and Keizer (1992) predicts bursting patterns. Despite these differences in behaviors, plateau fractions computed from most model equations depend monotonically on the glucose-dependent parameter  $\beta$ . For models with this property, different choices of  $\beta(g; \vec{v})$  should result in similar qualitative predictions for insulin release rates. In the case of the SRK model,  $\beta(g; \vec{v})$  is inversely proportional to the intracellular  $\text{Ca}^{2+}$  buffering rate,  $k_{Ca}$ . Regardless of which model is used, a comparison of experimentally measured buffering rates and those predicted by the fit  $\beta(g; \vec{v})$  obtained in Section 3 could be used to validate some of the assumptions made to develop the model equations.

The theoretical results presented here rely on a model for uncoupled  $\beta$ -cells whereas the experimental data for rates of insulin release are from intact islets. The effects of cell-cell coupling on the rates of insulin release from islets have not been measured experimentally. Numerical studies on the coupled  $\beta$ -cell model developed by Sherman and Rinzel (1992) have revealed that gap junction coupling tends to increase the plateau fraction of individual cells within the islet. Whether this translates into an increase in the rates of insulin secretion remains to be verified. If coupled  $\beta$ -cell models are to be used for predicting the rates

of insulin release then the effective plateau fractions should be computable directly from such models. In particular, a physiologically accurate model should, for example, mimic the experimentally observed fractional islet activity  $A(g)$  at intermediate glucose concentrations. We thank Arthur Sherman for references demonstrating inhibition or abolition of insulin secretion during BEA. This work was supported by the Natural Sciences and Engineering Research Council of Canada (R.M.M., Grant 5-84559) and by the National Science Foundation (M.P., EPSCoR Grant OSR-93-50-546).

## LITERATURE

- Ashcroft, S.J.H., J.M. Bassett and P.J. Randle. 1972. Insulin secretion mechanisms and glucose metabolism in isolated islets. *Diabetes (Suppl. 2)* **21**, 538–545.
- Ashcroft, F. and P. Rorsman. 1989. Electrophysiology of the pancreatic  $\beta$ -cell. *Prog. Biophys. Mol. Biol.* **54**, 87–143.
- Atwater, I., A. Goncalves, A. Herchuelz, P. Lebrun, W.J. Malaisse, E. Rojas and A. Scott. 1984. Cooling dissociates glucose-induced insulin release from electrical activity and cation fluxes in rodent pancreatic islets. *J. Physiol. (Lond.)* **348**, 615–627.
- Atwater, I., B. Ribalet and E. Rojas. 1978a. Cyclic changes in potential and resistance of the  $\beta$ -cell membrane induced by glucose in islets of Langerhans from mouse. *J. Physiol. (Lond.)* **278**, 117–139.
- Atwater, I., B. Ribalet and E. Rojas. 1978b. Mouse pancreatic  $\beta$ -cells: tetraethylammonium blockage of the potassium permeability increase induced by depolarization. *J. Physiol. (Lond.)* **288**, 561–574.
- Atwater, I., C.M. Dawson, B. Ribalet and E. Rojas. 1978. Potassium permeability activated by intracellular calcium ion concentration in the pancreatic  $\beta$ -cell. *J. Physiol. (Lond.)* **288**, 575–588.
- Atwater, I., C.M. Dawson, A. Scott, G. Eddelstone and E. Rojas. 1980. The nature of the oscillatory behaviour in electrical activity from pancreatic  $\beta$ -cell. *Horm. and Metab. Res. (Suppl.)* **10**, 100–107.

- Beigelman, M., B. Ribalet and I. Atwater. 1977. Electrical activity of mouse pancreatic beta-cells: II. Effects of glucose and arginine. *J. Physiol. (Paris)* **73**, 201–217.
- Bokvist, K., P. Rorsman and P.A. Smith. 1990. Block of ATP-regulated and  $\text{Ca}^{2+}$ -activated  $\text{K}^+$  channels in mouse pancreatic  $\beta$ -cells by external tetraethylammonium and quinine. *J. Physiol. (Lond.)* **423**, 327–342.
- Chay, T.R. and J. Keizer. 1983. Minimal model for membrane oscillations in the pancreatic  $\beta$ -cell. *Biophys. J.* **42**, 181–189.
- Cook, D.L. 1984. Electrical pacemaker mechanisms of pancreatic islet cells. *Federation Proc.* **43**, 2368–2372.
- Cook, D.L., L.S. Satin and W. Hopkins. 1991. Pancreatic  $\beta$ -cells are bursting, but how? *Trends in Neurosci.* **14**, 411–414.
- Dean, P.M. and E.K. Matthews. 1970a. Glucose-induced electrical activity in pancreatic islet cells. *J. Physiol. (Lond.)* **210**, 255–264.
- Dean, P.M. and E.K. Matthews. 1970b. Electrical activity in pancreatic islet cells: effects of ions. *J. Physiol. (Lond.)* **210**, 265–275.
- de Vries, G., R.M. Miura and M. Pernarowski. 1994. Analysis of models of pancreatic  $\beta$ -cells exhibiting temporal pattern formations. In *Pattern Formation: Symmetry Methods and Applications*, J. Chadam, M. Golubitsky, W. Langford and B. Wetton (Eds). Providence: American Mathematical Society. In press.
- Fatherazi, S. and D.L. Cook. 1991. Specificity of tetraethylammonium and quinine for three K channels in insulin-secreting cells. *J. Membrane Biol.* **120**, 105–114.
- Gembal, M., P. Gilon and J. Henquin. 1992. Evidence that glucose can control insulin release independently from its action on ATP-sensitive  $\text{K}^+$  channels in mouse B cells. *J. Clin. Invest.* **89**, 1288–1295.
- Gilon, P., R.M. Shepherd and J. Henquin. 1993. Oscillations of secretion driven by oscillations of cytoplasmic  $\text{Ca}^{2+}$  as evidenced in single pancreatic islets. *J. Biol. Chem.* **268**, 22265–22268.
- Henquin, J. 1990a. Glucose-induced electrical activity in  $\beta$ -cells, feedback control of ATP-sensitive  $\text{K}^+$  channels by  $\text{Ca}^{2+}$ . *Diabetes* **39**, 1457–1460.

- Henquin, J. 1990b. Role of voltage- and  $\text{Ca}^{2+}$ -dependent  $\text{K}^+$  channels in the control of glucose-induced electrical activity in pancreatic  $\beta$ -cells. *Pflüegers Arch.* **416**, 568–572.
- Henquin, J.C. and H.P. Meissner. 1984. Effects of theophylline and dibutyryl cyclic adenosine monophosphate on the membrane-potential of mouse pancreatic  $\beta$ -cells. *J. Physiol. (Lond.)* **351**, 595–612.
- Hodgkin, A.L. and A.F. Huxley. 1952. A quantitative description of membrane current and its application to conduction and excitation in nerve. *J. Physiol. (Lond.)* **117**, 500–544.
- Hopkins, W., L.S. Satin and D.L. Cook. 1991. Inactivation kinetics and pharmacology distinguish two calcium currents in mouse pancreatic  $\beta$ -cells. *J. Membrane Biol.* **119**, 229–239.
- Keizer, J. and P. Smolen. 1991. Bursting electrical activity in pancreatic  $\beta$  cells caused by  $\text{Ca}^{2+}$ - and voltage-inactivated  $\text{Ca}^{2+}$  channels. *Proc. Natl. Acad. Sci.* **88**, 3897–3901.
- Meissner, H.P. and M. Preissler. 1979. Glucose-induced changes in the membrane potential of pancreatic B cells: their significance for the regulation of insulin release. In *Treatment of Early Diabetes*, R.A. Camerini-Davalos and B. Hanover (Eds), pp. 97–107. New York: Plenum.
- Meissner, H.P. and M. Preissler. 1980. Ionic mechanisms of the glucose-induced membrane potential changes in  $\beta$ -cells. *Horm. and Metab. Res. (Suppl.)* **10**, 91–99.
- Meissner, H.P. and H. Schmelz. 1974. Membrane potential of beta-cells in pancreatic islets. *Pflüegers Arch.* **351**, 195–206.
- Ozawa, S. and O. Sand. 1986. Electrophysiology of endocrine cells. *Physiol. Rev.* **66**, 887–952.
- Pernarowski, M., R.M. Miura and J. Kevorkian. 1991. The Sherman-Rinzel-Keizer model for bursting electrical activity in the pancreatic  $\beta$ -cell. In *Differential Equation Models in Population Dynamics and Physiology*, S. Busenberg and M. Martelli (Eds), pp. 34–53. Berlin: Springer-Verlag.
- Pernarowski, M., R.M. Miura and J. Kevorkian. 1992. Perturbation techniques for models

- of bursting electrical activity in pancreatic  $\beta$ -cells. *SIAM J. Appl. Math.* **52**, 1627–1650.
- Rinzel, J., T.R. Chay, D. Himmel and I. Atwater. 1986. Prediction of the glucose-induced changes in membrane ionic permeability and cytosolic  $Ca^{2+}$  by mathematical modelling. *Adv. Exp. Med. Biol.* **211**, 247–263.
- Rorsman, P. and G. Trube. 1986. Calcium and delayed potassium currents in mouse pancreatic  $\beta$ -cells under voltage-clamp conditions. *J. Physiol. (Lond.)* **374**, 531–550.
- Rosario, L.M., I. Atwater and E. Rojas. 1985. Membrane potential measurements in islets of Langerhans from ob/ob obese mice suggest an alteration in  $[Ca]^{2+}$ -activated  $K^+$  permeability. *Q. J. Exp. Physiol.* **70**, 137–150.
- Santos, R.M., L.M. Rosario, A. Nadal, J. Garcia-Sancho, B. Soria and M. Valdeolmillos. 1991. Widespread synchronous  $[Ca^{2+}]_i$  oscillations due to bursting electrical activity in single pancreatic islets. *Pflüegers Arch.* **418**, 417–422.
- Satin, L.S. and D.L. Cook. 1988. Evidence for two calcium currents in insulin-secreting cells. *Pflüegers Arch.* **411**, 401–409.
- Satin, L.S. and D.L. Cook. 1989. Calcium current inactivation in insulin-secreting cells is mediated by calcium influx and membrane depolarization. *Pflüegers Arch.* **414**, 1–10.
- Scott, A.M., I. Atwater and E. Rojas. 1981. A method for the simultaneous measurement of insulin release and B cell membrane potential in single mouse islets of Langerhans. *Diabetologia* **21**, 470–475.
- Sherman, A. and J. Rinzel. 1992. Rhythmogenic effects of weak electrotonic coupling in neuronal models. *Proc. Natl. Acad. Sci.* **89**, 2471–2474.
- Sherman, A., J. Rinzel and J. Keizer. 1988. Emergence of organized bursting in clusters of pancreatic  $\beta$ -cells by channel sharing. *Biophys. J.* **54**, 411–425.
- Smolen, P. and J. Keizer. 1992. Slow voltage inactivation of  $Ca^{2+}$  currents and bursting mechanisms for the mouse pancreatic beta-cell. *J. Membrane Biol.* **127**, 9–19.
- Strumwasser, F. 1968. Membrane and intracellular mechanism governing endogenous activity in neurons. In *Physiological and Biochemical Aspects of Nervous Integration*, F.D. Carlson (Ed), pp. 329–342. Englewood Cliffs: Prentice-Hall.



- Valdeolmillos, M., R.M. Santos, D. Contreras, B. Soria and L.M. Rosario. 1989. Glucose-induced oscillations of intracellular  $\text{Ca}^{2+}$  concentration resembling bursting electrical activity in single mouse islets of Langerhans. *FEBS Lett.* **259**, 19–23.
- Wollheim, C.B. and W.F. Pralong. 1990. Cytoplasmic calcium ions and other signalling events in insulin secretion. *Biochem. Soc. Trans.* **18**, 111–114.

Figure 1. Insulin release rates and plateau fractions in  $\beta$ -cell islets. (a) Experimental rate of insulin release as a function of glucose concentration. (b) Experimental plateau fractions as a function of glucose concentration. Data taken from authors indicated in legends, cf. Table 1.

Figure 2. Effective plateau fraction as a function of normalized insulin release rate. Data taken from authors indicated in legends, cf. Table 1.

Figure 3. Plateau fractions as a function of glucose concentration. Solid lines indicate theoretically obtained values for  $\hat{\rho}$  from the SRK model. Note the jumps in both the experimental and theoretical values of the plateau fraction at  $g_t = 5$  mM and  $g_s = 16.6$  mM. Solutions of the SRK equations exhibited chaotic behavior for glucose values between the vertical dashed lines. Relationship between the glucose concentration,  $g$ , and the buffering rate,  $k_{Ca}$ , is approximated by (11) using  $p = 3$ . Data taken from authors indicated in legends, cf. Table 1.

Figure 4. Effective plateau fraction as a function of glucose concentration. For the case  $p = 3$ , the effective plateau fraction,  $\rho_f$ , for the SRK model is plotted against glucose concentration. The difference between this graph and the graph in Figure 3 occurs in the glucose range 5 to 9.4 mM where the multiplicative factor  $A$  in (2) increases from zero to one. Data taken from authors indicated in legends, cf. Table 1.

Figure 5. Experimental and theoretical insulin release rates obtained from experimental and theoretical plateau fractions. Solid lines indicate release rates obtained using plateau fractions computed from the SRK model of BEA in  $\beta$ -cells. Data taken from authors indicated in legends, cf. Table 1.